Int. J. Electrochem. Sci., 7 **(2012)** 4418 - 4431

International Journal of
ELECTROCHEMICAL
SCIENCE
www.electrochemsci.org

Electrochemical Corrosion Inhibition of Al-Si Alloy in Phosphoric Acid

M.A. Ameer[*] *, A.A.Ghoneim and A.M. Fekry*

Chemistry Department, Faculty of Science, Cairo University, Giza-12613, Egypt.
[*]E-mail: mameer_eg@yahoo.com

Received: 9 March 2012 / *Accepted:* 27 March 2012 / *Published:* 1 May 2012

Electrochemical corrosion inhibition of aluminum die casting alloy (A383) in H_3PO_4 has been studied using different electrochemical techniques. The results of electrochemical impedance spectroscopy (EIS) and potentiodynamic polarization measurements confirm the inhibition effects of K_2CrO_4 which describe the increase in the effectiveness of a corrosion inhibitor in the presence of 0.1M K_2CrO_4 in 0.5 M H_3PO_4. The results indicated that both concentration and the immersion time affect the inhibition efficiency (IE%). Langmuir adsorption isotherm was found to fit well with the experimental data. The obtained results were confirmed by surface examination using scanning electron microscope.

Keywords: A383; Polarization; EIS; SEM; acid inhibition

1. INTRODUCTION

Aluminium–silicon (Al–Si) alloys constitute a class of material that is being used to replace cast iron parts in automobile engines. Benefits of the replacement to the car industries include resistance to corrosion, well thermal conductivity, and moderate costs. Aluminium is used specifically to reduce weight compared to steel, and is alloyed with silicon to increase the strength of the material. It is well known that silicon solidifies in a separate hard phase, which becomes the load-bearing surface [1]. Aluminium (Al) die casting alloys have a specific gravity of approximately 2.7 g/cc, placing them among the lightweight structural metals. The majority of die castings produced worldwide are made from aluminium alloys. Alloy A383 offers improved resistance to hot cracking (strength at elevated temperatures). Aluminium die casting alloys are lightweight, offer good corrosion resistance, ease of casting, good mechanical properties and dimensional stability. Although a variety of aluminium alloys made from primary or recycled metal can be die cast, most designers select A 383 as one of the standard alloys.

Aluminium relies on the formation of a compact, adherent passive oxide film for its corrosion immunity in various environments. However, this surface film is amphoteric and dissolves substantially when it is exposed to high concentrations of acids or bases. Phosphoric acid ($H_3 PO_4$) is widely used for acid cleaning and electropolishing of aluminium [2], but it still shows strong corrosiveness on aluminium and its alloys. Therefore, it is necessary to seek inhibitors for the corrosion of aluminium in H_3PO_4. An extensive review of the literature reveals that very little attention has been paid to inhibition studies on aluminium alloy in H_3PO_4. With respect to the inorganic inhibitors, Cr^{6+} compounds act as the effective and inexpensive corrosion inhibitors for aluminium in H_3PO_4. In 1935, Rohrig [3] first reported that sodium chromate (Na_2CrO_4) is a good corrosion inhibitor for aluminium in 20% H_3PO_4. In 1980s, some authors [4, 5] studied the inhibition effect of potassium chromate (K_2CrO_4) and potassium dichromate ($K_2Cr_2O_7$) on the corrosion of aluminium in H_3PO_4 using the weight loss method. The use of inhibitors for the control of corrosion of metals and alloys which are in contact with aggressive environment is an accepted practice. The use of corrosion inhibitor is one of the most practical methods for protecting the corrosion of metal. As a result, corrosion inhibitors for hydrochloric acid, phosphoric acid and sulfuric acid have attracted increasing attention due to their extended applications [6-10]. The protection of metals against corrosion by H_3PO_4 has been the subject of much study since it has been used in many industrial processes especially in fertilizer production [11-15].

The main aim of this research work is to study the electrochemical behavior of aluminium die casting alloy (A383) at different immersion time and concentrations of $K_2Cr_2O_7$ in naturally aerated 0.5M H_3PO_4 solutions using electrochemical techniques and surface examination.

2. EXPERIMENTAL

The aluminium die casting alloy (A383) rod was tested in the present study with its cross-sectional area of 0.785 cm^2. The chemical composition of the alloy, as given by the supplier, is listed in Table 1.

Table 1. The chemical composition of A383 wt %

Al	Si	Zn	Cu	Fe	Mn	Mg	Sn	Ni	Cr	Pb	Na	Ti
79.952	10.614	2.91	2.52	0.918	0.21	0.057	0.052	0.05	0.069	0.052	0.041	0.038

The test aqueous solutions contained 0.5M H_3PO_4 (BDH) and K_2CrO_4 with different concentrations. Triple distilled water was used for preparing all solutions. In all measurements, mechanically polished electrode was used. Polishing was affected using successively finer grade of emery papers (600-1200 grade). Polarization and electrochemical impedance spectroscopy (EIS)

measurements were carried out using the electrochemical workstation IM6e Zahner-electrik GmbH, Meβtechnik, Kronach, Germany. The excitation AC signal had amplitude of 10 mV peak to peak in a frequency domain from 0.1 Hz to 100 kHz. The EIS was recorded after reading a steady state open-circuit potential. The scanning was carried out at a rate 30 $mVmin^{-1}$ over the potential range from – 1500 to + 1000 mV vs. saturated calomel electrode (SCE). Prior to the potential sweep, the electrode was left under open-circuit in the respective solution for ~ 2 hours until a steady free corrosion potential was recorded. Corrosion current density, i_{corr}, which is equivalent to the corrosion rate, is given by the intersection of the Tafel lines extrapolation. Because of the presence of a degree of nonlinearity in the Tafel slope part of the obtained polarization curves, the Tafel constants were calculated as a slope of the points after E_{corr} by ± 50 mV using a computer least-squares analysis. i_{corr} were determined by the intersection of the cathodic Tafel line with the open-circuit potential. For surface examination, the electron microscope used is JEOL-JEM-100s type with magnification of 100x.

3. RESULTS AND DISCUSSION

3.1. Electrochemical impedance measurements

3.1.1. Effect of K_2CrO_4 concentration

Electrochemical impedance (EIS) is a technique with small perturbative signal and the surface damage of the sample is very little. Besides, the corrosion mechanism can be estimated by analyzing the measured electrochemical impedance spectrum.

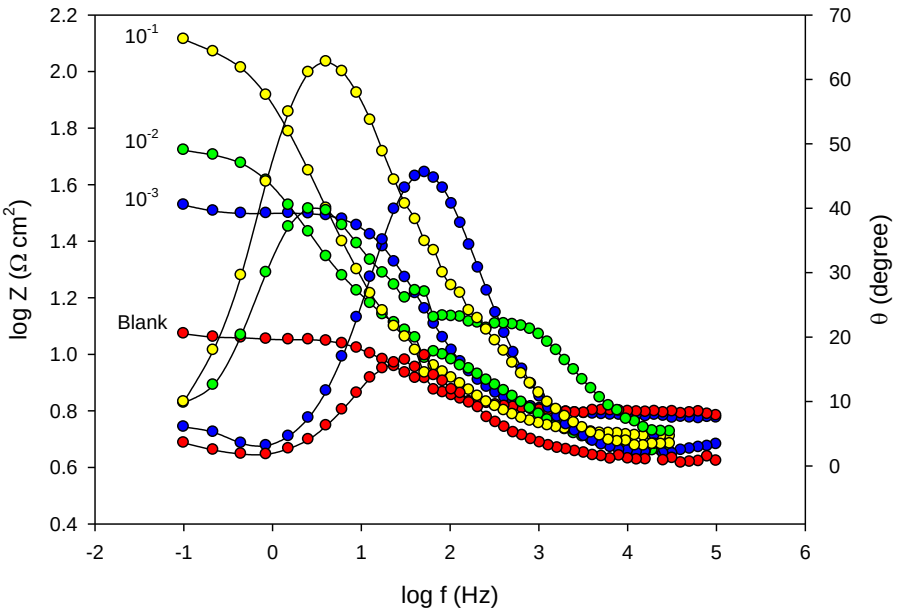

Figure 1. Bode plots of A383 in 0.5 M H_3PO_4 without and with different concentrations of K_2CrO_4 .

Figs. 1 shows the EIS data for the A383 traced at the rest potential in 0.5 M H_3PO_4 solutions with and without different concentrations (10^{-3} – 10^{-1} M) of K_2CrO_4 after 2h. The figure manifested typical of Randles element and inductive loops can be explained by the occurrence of adsorbed intermediate on the surface. Therefore, adsorbed intermediate species such as Al^{+}_{ads} and Al^{3+}_{ads} might be involved in Al dissolution process [16]. The proposed equivalent circuit manifested in Fig. 2, is used to analyze the impedance spectra of A383 in H_3PO_4 solutions without and with K_2CrO_4. The model includes the solution resistance R_s, in a series combination of two resistances, R_1 *and* R_2, which are in parallel with each of inductance, *L*, capacitance, C and the constant phase element, Q. Contribution to the total impedance at intermediate frequencies comes mainly from inductive component in parallel.

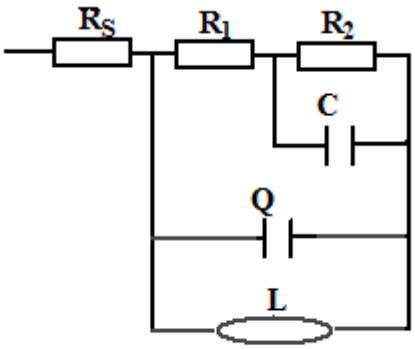

Figure 2. Equivalent circuit model representing two time constants for an electrode/electrolyte solution interface.

The inductor arise from adsorption effects could be define as ($L = R\tau$) where τ is the relaxation time for adsorption on electrode surface. The low frequency locus displays the characteristics of parallel RC circuit. This circuit includes another constant phase element (Q) which is placed in parallel to R_1 and R_2.The CPE is used in this model to compensate for nonhomogeneity in the system and is defined by two values, *Q* and α. In order to understand the physical significance of each element of the electronic equivalent circuit, it can be considered that R_S corresponds to the solution resistance; R_1 and R_2 correspond to the polarization resistance of the surface of the samples and oxide film formations, respectively. The C and Q correspond to the capacitances of the experimentally examined samples and their oxide layer formation, respectively. The impedance of CPE is representing by [17]:

$$Z_{CPE} = Q^{-1}(i\omega)^{-\alpha} \qquad (1)$$

where $i = (-1)^{1/2}$, ω is frequency in rad s^{-1}, $\omega = 2\pi f$ and *f* is the frequency in Hz. If α equals one, the impedance of CPE is identical to that of a capacitor, $Z_c = (i\omega C)^{-\alpha}$, and in this case *Q* gives a pure capacitance (*C*). Computer fitting of the spectrum allows evolution of the elements of the circuit analogue. The aim of the fitting procedure is to find those values of the parameters which best describe the data, i.e., the fitting model must be consistent with the experimental data. The experimental and

computer fit results of Nyquist plot and Bode plots (impedance and θ) for A383 in 0.5M H_3PO_4 containing different concentration of K_2CrO_4 is demonstrated in Figs.. It was found that the fit results were consistent with the experimental data within 5% of errors. The fit results for different concentrations of K_2CrO_4 in 0.5M H_3PO_4 are given in Table 2.

Table 2. Equivalent circuit parameters of A383 in 0.5 M H_3PO_4 solutions without and with different concentration of K_2CrO_4

Conc.of K_2CrO_4 (M)	R_1 (Ω cm^2)	C (μF cm^{-2})	R_2 (Ω cm^2)	Q (μF cm^{-2})	α	L (kH)	Rs (Ω)	IE%
0.000	0.8	90.9	19.6	101.9	0.85	0.45	3.0	--
0.001	1.8	77.1	30.9	99.7	0.86	0.65	3.4	37.5
0.010	20.9	65.9	90.5	88.9	0.84	7.7	5.9	81.6
0.050	27.9	56.4	113.2	84.2	0.85	8.8	6.2	85.5
0.100	12.9	55.4	372.6	45.5	0.83	9.20	6.7	94.7

The data indicate that decreasing concentration of K_2CrO_4 from 10^{-1} to 10^{-3} M decrease values of R_T, L and increase the constant phase, *Q*, which can be attributed to the adsorption process. The calculated values of α are found to be within the value of 0.85 which explains a type of non-homogeneity due to presence of chromate and/or hydrogen ions that turn aluminium surface rough or porous. Fig. 3 shows the variations of the total resistance, $R_T = (R_1 + R_2)$, with chromate concentrations in 0.5M H_3PO_4. The R_T gives an indication for the system resistivity towards corrosion and is inversely proportional to the corrosion rate. These curves represent rapid increase of the R_T with increasing K_2CrO_4concentrations.

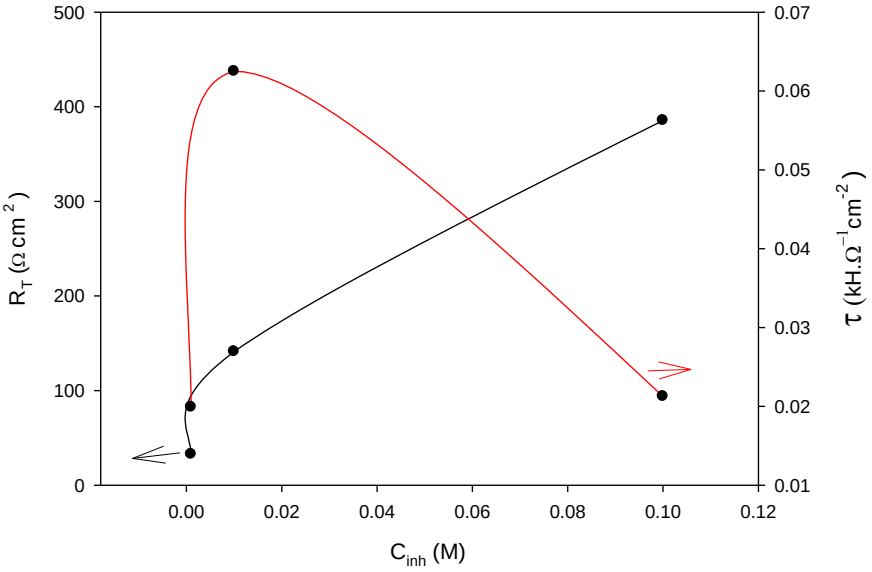

Figure 3. The variations of the total resistance, R_T , and relaxation time, τ , of A383 with chromate concentrations in 0.5M H_3PO_4.

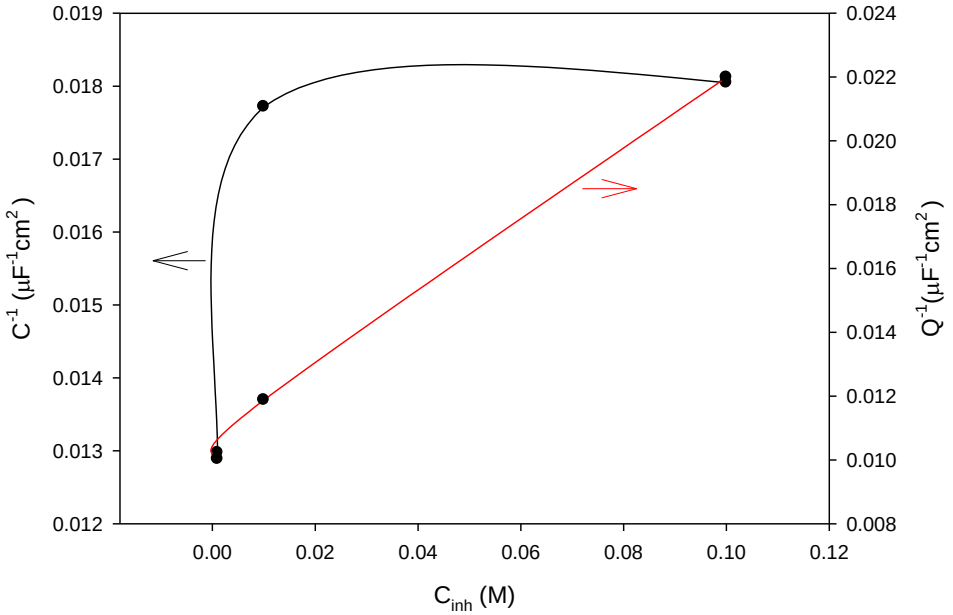

Figure 4. The variation of C^{-1} and Q^{-1} values of A383 with concentration of K_2CrO_4 in 0.5 M H_3PO_4 solutions.

Fig. 3 shows the variations of the relaxation time, $\tau = L/R_T$, with K_2CrO_4 concentrations in 0.5M H_3PO_4. Since the relaxation time is a measure of the rate at which a disequilibrium distribution decays toward an equilibrium distribution. The plot is remarkably observed that the relaxation time increases with increasing K_2CrO_4 concentration up to a critical value after which the τ values decrease again. The critical K_2CrO_4 concentration is 10^{-2} M. Fig.4 represents the variation of C^{-1} and Q^{-1} values of A383 with concentration of K_2CrO_4 in 0.5 M H_3PO_4 solutions. The data indicates that both C^{-1} and Q^{-1} increase with increasing K_2CrO_4 concentrations. The unique chemical and electronic properties of the oxo-compounds of chromium, Cr (valence electronic structure $3d^5\ 4s^1$) [18] gives them a seemingly unique ability to inhibit corrosion in ferrous and nonferrous materials. The electronic properties of Cr allow for very different behaviors for the oxo- and hydroxocompounds of Cr^{6+} and Cr^{3+}. The tetrahedral, d^0, hexavalent oxoanion compounds of chromium (chromate, dichromate, bichromate, and chromic acid) dissolve as stable complexes in water, transport easily, and adsorb on oxide surfaces. The octahedral, d^3, trivalent compounds of Cr form very stable, kinetically inert refractory oxides. Bulk Cr^{3+} hydroxides form by sol-gel polymerization, giving rise to well Cr^{6+} is readily hydrolyzed in aqueous solution and exists as an oxoanion in all but the most acidic conditions. Hydrolysis of Cr^{6+} is directly related to corrosion inhibition because it affects speciation, adsorption, transport, and condensation processes, which all have roles in chromate corrosion protection. Unfortunately, hydrolysis and subsequent speciation of Cr^{6+} oxoanions compounds is often neglected in studies of inhibition [19]. Recent investigation of corrosion protection by chromates has focused on a number of specific working hypotheses regarding the mechanisms of inhibition. They can be condensed to the following statements: Cr^{6+} oxoanions being highly soluble and very mobile in solution, are transported to sites of localized corrosion where they are reduced to Cr^{3}+ and irreversibly

adsorbed at metal surfaces where they inhibit oxygen reduction; inhibit pit initiation of Al and dissolution of active intermetallic phases in Al alloys; modify the chemical composition of the surface of passive oxides and passivated intermetallic phases by adsorption and buffering; adsorb on aluminum oxides, lowering the zeta potential, thereby discouraging adsorption of anions chloride, which promote dissolution and destabilization of protective oxides[18].

3.1.2. Effect of immersion time

In these experiments, the immersion of A383 alloy was carried out continuously in 0.5 M H_3PO_4 solution without and with 10^{-1}M K_2CrO_4 .The specimens were suspended in the test solution up to 96 h. The EIS scans as Bode plots and Nyquist at different immersion times are given in Figs. 5a,b and 6a,b for A 383 respectively. It can be seen that these diagrams show resistive regions at high and low frequencies and inductive contribution at intermediate frequencies. The impedance (|Z|) as well as the phase shift θ is clearly found to depend on immersion time. It is found that R_T increases with immersion time while each of C and Q decreases. The Equivalent circuit parameters of A383 in 0.5 M H_3 PO_4 solution without and with 10^{-1}M K_2CrO_4 are tabulated in Table 3.

Table 3. Equivalent circuit parameters and inhibition efficiency of A383 in 0.5 M H_3 PO_4 solutions in+ 10^{-1} M K_2CrO_4 at different immersion time.

Time	R_1	C	R_2	Q	α	L	R_s	IE%
(h)	(Ω cm^2)	(μF cm^{-2})	(Ω cm^2)	(μF cm^{-2})		(kH)	(Ω)	
0.00	28.8	68.0	130.4	29.9	0.82	1.24	8.65	85.6
0.25	21.4	66.8	193.6	38.9	0.85	2.87	8.71	90.2
0.50	21.3	63.8	285.5	42.2	0.81	5.94	8.62	93.6
1.0	17.7	58.9	370.4	43.8	0.80	7.41	8.13	95.2
2.0	12.9	55.4	372.6	45.5	0.83	9.18	6.66	94.7
3.0	12.5	52.8	404.9	46.4	0.81	10.81	6.74	94.6
5.0	11.9	42.2	565.4	47.9	0.83	12.83	6.88	95.3
24	11.2	39.2	688.5	50.9	0.84	14.49	7.52	94.5
96	10.2	29.8	1168.1	51.3	0.85	16.39	8.08	95.5

However, at any immersion time the values of R_T are always higher for A383 in 0.5 M H_3PO_4 solution with 10^{-1}M K_2CrO_4 as compared to A383 alloy in blank solution suggesting that K_2CrO_4 makes A383 alloy much more passive than in the blank.Fig.7, represents the variation of total resistance with immersion time in 0.5 M H_3 PO_4 solution without and with 10^{-1}M K_2CrO_4. The results were confirmed using surface examination. All corroded specimens were rinsed gently with distilled water, dried and stored in a desiccator for several days before they were examined by scanning electron microscopy (SEM). Figure 8(a, b) represents an example for the SEM image for tested electrode in 0.5M H_3PO_4 (blank) without K_2CrO_4 (Fig. 8a), and with 10^{-1} M K_2CrO_4 (Fig. 8b). it is clear from the figure that for 10^{-1} M K_2CrO_4 in 0.5 M H_3PO_4 the image is smoother than blank.

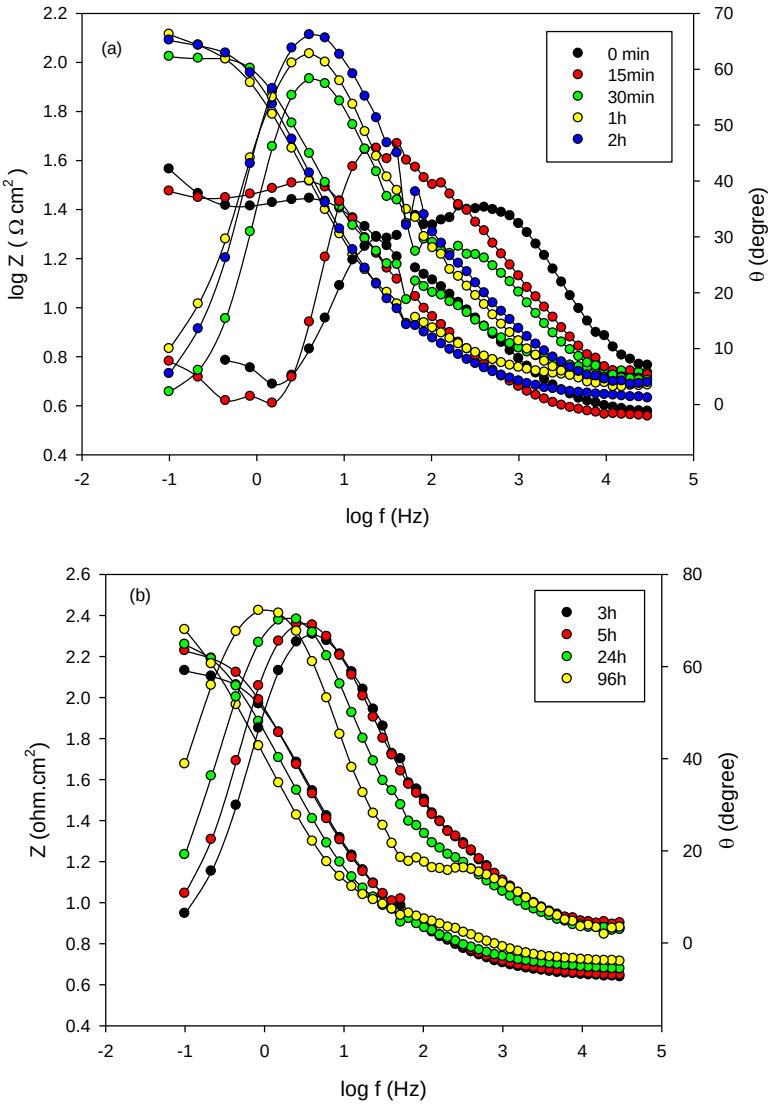

Figure 5. (a,b) Bode plots of A383 in 0.5 M H_3PO_4 solution without and with 0.1M K_2CrO_4 at different immersion times.

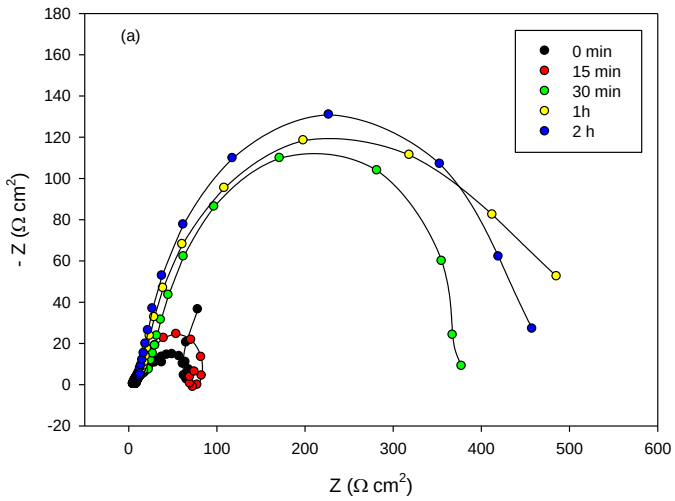

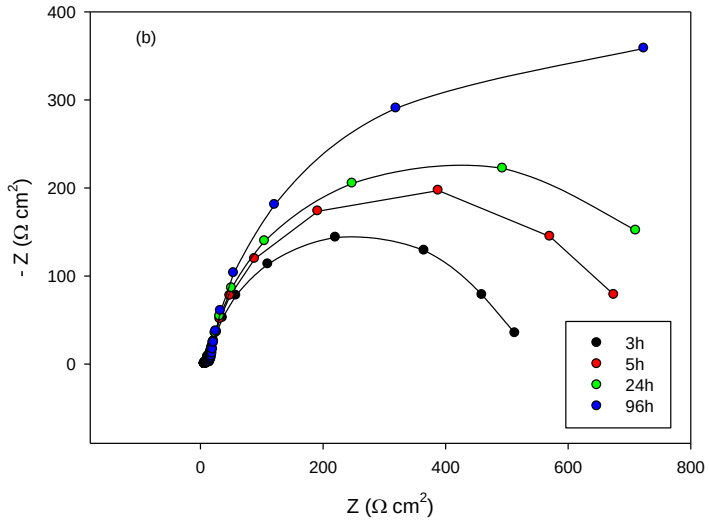

Figure 6. (a,b) Nyquist plots of A383 in 0.5 M H_3PO_4 solution without and with 0.1M K_2CrO_4 at different immersion times.

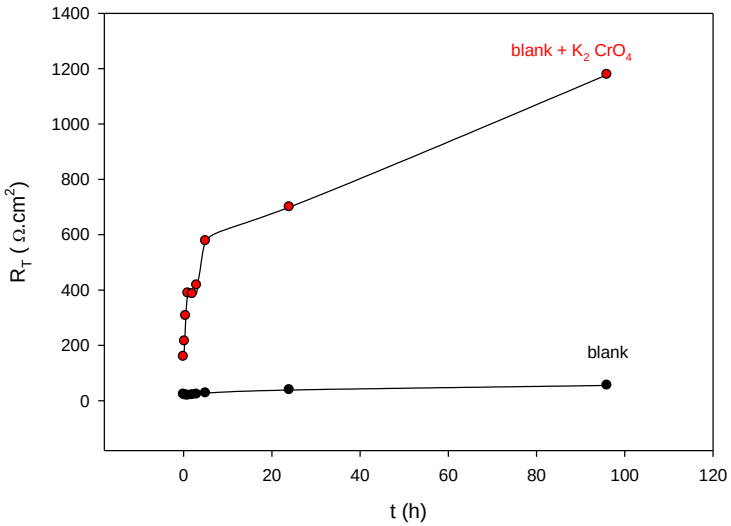

Figure 7. The variations of the total resistance, R_T,of A383 with immersion time in 0.5M H_3PO_4 without and with 0.1M K_2CrO_4.

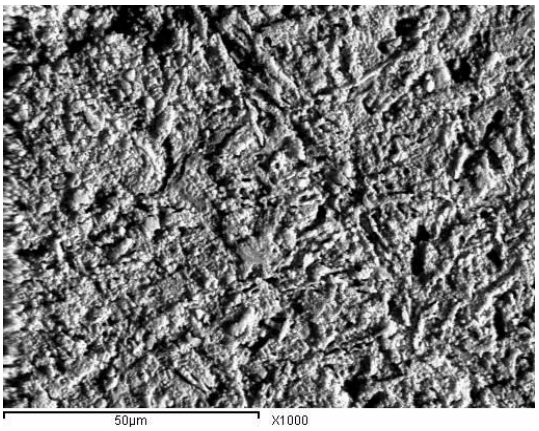

A

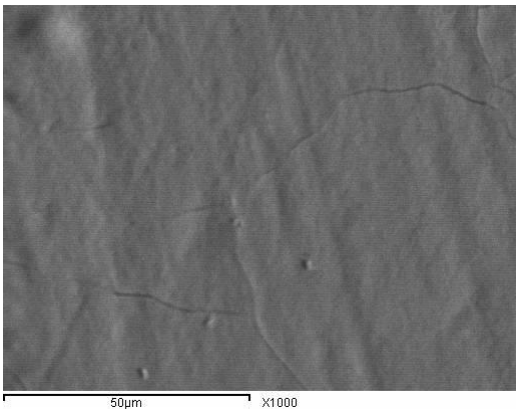

B

Figure 8. SEM image for tested electrode in 0.5M H_3PO_4 (blank) without K_2CrO_4 (Fig. 8a), and with 0.1 M K_2CrO_4 (Fig. 8b).

3.2. Potentiodynamic Polarization Measurements

In this part the potentiodynamic polarization behavior of A383 was studied in relation to nature and concentration of the aqueous solutions. Fig.9 shows a typical linear sweep potentiodynamic trace for A383 in 0.5 M H_3PO_4 without and with different concentrations of K_2CrO_4 solutions. The polarization curves were obtained for different concentrations of K_2CrO_4 in 0.5 M H_3PO_4 solution. It is noticed that the corrosion potential shifts towards more anodic potential with presence of K_2CrO_4 and as the concentration increases as shown in Table 4. A difference of 400 mV is measured between the corrosion potential of the alloy in 10^{-3} and in 10^{-1} M K_2CrO_4. In the anodic range a current plateau is observed. For the tested A383 the estimated i_{corr} is illustrated in Fig. 10 as a function of the concentration of K_2CrO_4 in 0.5M H_3PO_4. The results indicate clearly that (i_{corr}) is dependent on the concentration. The results indicate that K_2CrO_4acts as an anodic inhibitor in 0 .5 M H_3PO_4. It is important to note that in the anodic domain, there is a strong decrease of the anodic current density after adding K_2CrO_4 in H_3PO_4.

Table 4. Corrosion parameters of A383 in 0.5 M H_3 PO_4 solutions containing different concentration of K_2CrO_4

Conc.of K_2CrO_4 (M)	$-E_{corr}$ (mV)	i_{corr} (µA cm^{-2})	$-\beta_c$ (mV/dec)	β_a (mV/dec)	IE%
0.000	1280.0	805.1	197	174	--
0.001	627.4	566.8	181	170	29.5
0.050	539.4	77.0	130	164	90.4
0.010	453.8	75.4	140	150	90.6
0.100	294.7	48.5	180	148	93.9

The electrochemical corrosion parameters of corrosion current densities ((i_{corr}), corrosion potential (E_{corr}), anodic Tafel slope (β_a) and cathodic Tafel slope (β_c) are estimated by extrapolating both cathodic and anodic linear regions back to the corrosion potential,

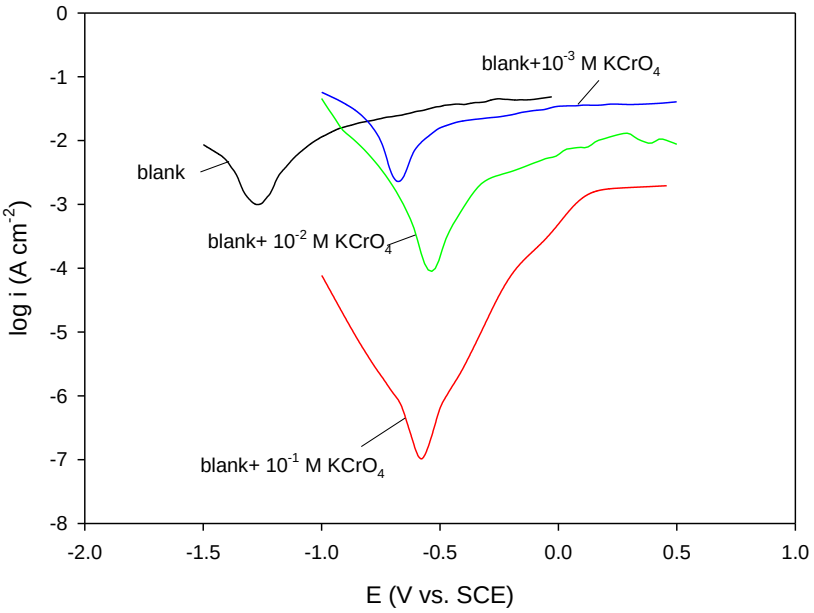

Figure 9. Potentiodynamic polarization curves of A383 in 0.5 M H_3PO_4 without and with different concentrations of K_2CrO_4.

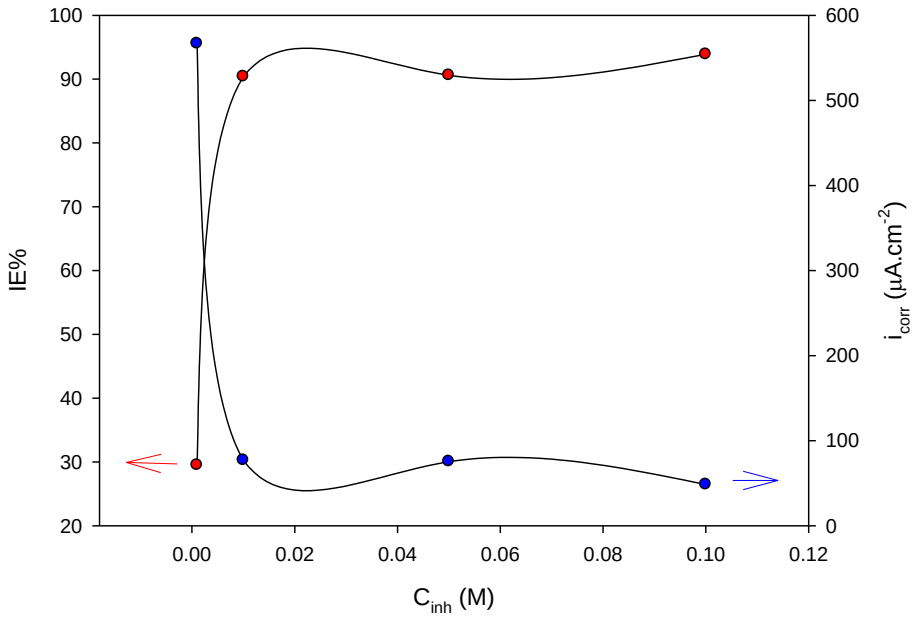

Figure 10. Variation of IE% and i_{corr} of A383 in 0.5 M H_3PO_4 without and with different concentrations of K_2CrO_4.

The electrochemical corrosion parameters and inhibition efficiency (IE) are listed in Table 4. Apparently, i_{corr} decreases considerably in the presence of K_2CrO_4, and decreases with increasing the inhibitor concentration. Correspondingly, IE increases with the inhibitor concentration, due to the increase in the blocked fraction of the electrode surface by adsorption. IE of 0.1M inhibitor reaches up

to the maximum of 93.9%, which indicates that K_2CrO_4 is a good inhibitor for aluminium in 0.5 M phosphoric acid. The presence of K_2CrO_4 shifts E_{corr} to positive, which further confirms that K_2CrO_4 acts as an anodic-type inhibitor [18]. In addition, there are no significant changes in Tafel slopes of βa and βc, which indicates that the presence of inhibitor does not change the aluminium corrosion mechanism. The corrosion parameters are given in Table 5 and the inhibition efficiency (IE %) are calculated, Table 4, from the following equation [20] :

$$IE\% = 1 - \frac{i_{inh}}{i_{corr}} \times 100 \qquad (2)$$

where i_{corr} and i_{inh} are the uninhibited and inhibited corrosion current densities, respectively. It can be seen from the experimental results derived from polarization curves that increasing K_2CrO_4concentration decreased i_{corr} at all of the studied concentrations. The change of cathodic and anodic Tafel slopes alters unremarkably in the presence of the inhibitor. This is indicative that the inhibitor acts by merely blocking the reaction sites of the metal surface without changing the anodic and cathodic reaction mechanisms. Both the anodic and cathodic current densities were decreased indicating that K_2CrO_4 suppressed both the anodic and cathodic reactions. Also it was found that the IE increases till 93.9% at 10^{-1} M K_2CrO_4 concentration as shown in Fig. 10.

3.3 Adsorption Isotherm

With regard to Langmuir adsorption isotherm, Eq. (3), it was found to fit well with the experimental data obtained. Where θ is the surface coverage (IE %) / 100) of the inhibitor on the Titanium alloy surface which is related to the concentration (C) of the inhibitor in the bulk of solution according to the following equation [21]:

$$\frac{C}{\theta} = \frac{1}{K_{ads}} + C \qquad (3)$$

K_{ads} is the adsorption-desorption equilibrium constant. By plotting C/θ versus C at 298K for the three inhibitors, straight lines were obtained as seen in Fig.11. From the intercepts, K_{ads} values were calculated for the adsorption process. A straight line is obtained on plotting c/h versus c as shown in Fig.11. Both linear correlation coefficient (r) (r = 0.9986) and slope (slope = 1.0535) are almost equal to 1, which indicates the adsorption of inhibitor obeys Langmuir adsorption isotherm. The adsorptive equilibrium constant (K) value calculated is 344.8 M^{-1}. Thermodynamic parameters are important to study the inhibitive mechanism. The standard free energy of adsorption (ΔG°_{ads}) related to the adsorptive equilibrium constant (K_{ads}) can be obtained from the following equation: [22]

$$\log K_{ads} = \log \frac{1}{55.5} + \frac{\Delta G^{\circ}_{ads}}{2.303RT} \qquad (4)$$

where R is the gas constant (8.314 J K^{-1} mol^{-1}), T the absolute temperature (K), the value 55.5 is the concentration of water in the solution expressed in M . The ΔG°_{ads} values are -13.517 kJ mol^{-1}.

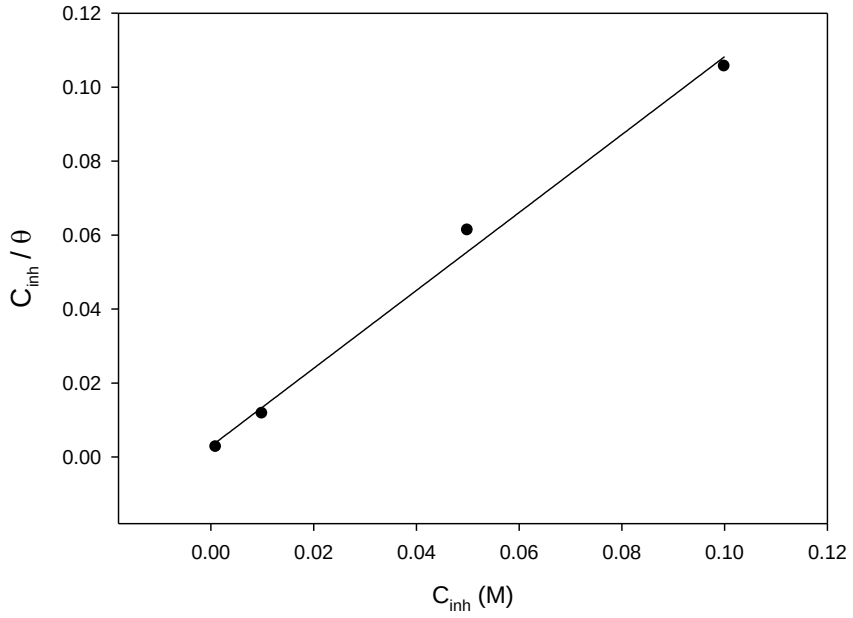

Figure 11. Langmuir isotherm adsorption mode of A383 at diferent concentration of K_2CrO_4 in 0.5 M H_3PO_4 solutions.

Generally, value of ΔG°_{ads} up to -20 kJ mol^{-1} is consistent with the electrostatic interaction between the charged molecules and the charged metal (physisorption), while the value more negative than -40 kJ mol^{-1} involves sharing or transfer of electrons from the inhibitor molecules to the metal surface to form a co-ordinate type of bond (chemisorption) [23]. In the present study, the value of ΔG° is less than -20 kJ mol^{-1} probably means that physical adsorption would take place.

4. CONCLUSIONS

Based on the results of potentiodynamic polarization and EIS measurements the following conclusions are drawn in this study:

- K2CrO4 acts as a good inhibitor for the Al-Si alloy in 0.5 M H3PO4 solution.
- Inhibition efficiency increases with the inhibitor concentration, and the maximum inhibition efficiency obtained from impedance and polarization is 94.7% and 93.9% respectively at 0.1M K2CrO4.
- The adsorption of K2CrO4 obeys Langmuir adsorption isotherm.
- K2CrO4 acts as an anodic inhibitor.
- The presence of K2CrO4 in 0.5 M H3PO4 solutions enhances RT values .
- The oxoanions of hexavalent chromium uniquely inhibit the corrosion of many metals and alloys and have been particularly useful for protecting the high strength aluminium alloys against corrosion.

- SEM suggesting that addition of K2CrO4inhibitor in the H3PO4 enhances the corrosion resistance of A 383 and this confirms the impedance and polarization results.

References

1. G. Pereira, A. Lachenwitzer, M. Kasrai, P.R. Norton , T.W. Capehart, T.A. Perryb, Y.T. Cheng, B. Frazer,P.U. Gilbert .*Tribology Letters*.26, 103(2007).
2. M.A. Amin, Q. Mohsen, O.A. Hazzai. *Mater. Chem. Phys*. 114, 908(2009).
3. H. Rohri. *Aluminium* .17 (1935) 559–562
4. G.N. Mu. *J. Chin. Soc. Corros. Prot*. 8, 335 (1988).
5. G.N. Mu. *Corros. Prot*. 9, 22, (1989).
6. K.F.Khaled. *Appl. Surf. Sci*. 230, 307(2004).
7. V. Branzoi, F. Golgovici, F. Branzoi. *Mat. Chem. Phys*.78, 122(2002).
8. A.S. Algaber, E.M. El-Nemma , M.M. Saleh. *Mater. Chem. Phys*. 86, 26(2004).
9. M.A. Migahed, H.M. Mohamed, A.M. Al-Sabagh. *Mater. Chem. Phys*. 80, 169 (2003).
10. M. Lashkari and M. Arshadi. Chem. Phys. 299, 131(2004).
11. A. Popova, M. Christov, S. Raicheva, E. Sokolova. *Corros*. *Sci.* 46, 1333(2004).
12. L. Wang. *Corros. Sci*. 43, 2281(2001).
13. E. Noor. *Corros. Sci*. 47, 33(2005).
14. L. Wang. *Corros. Sci*. 48, 608(2006).
15. M. Benabdellah, M. Benkaddour, B. Hammouti, M. Bendahhou, A. Aouniti. *Appl. Surf. Sci*. 252, 6212(2006).
16. M. Benabdellah, A. Aouniti, A. Dafali, B. Hammouti, M. Benkaddour, A. Yahyi, A. Ettouhami. *Appl. Surf. Sci*.252, 8341(2006).
17. U. Rammelt, G. Reinhard. *Electrochim. Acta* . 35, 1045(1990).
18. M.W.Kendig. *Corrosion*. 59, 379(2003).
19. 19.C.F. Baes, R.E.Mesmer. FL: Robert E. Kreiger Publishing Co., 1986.
20. D.D.Macdonald. *Electrochim. Acta*. 35, 1509(1990).
21. M.A.Ameer. *Materials Chemistry and Physics*. 122, 321(2010).
22. M.A.Ameer, A.M. Fekry. *Progress in Organic Coating*. 71, 343(2011).
23. F.Bentiss, M. Lebrini, M. Lagrenée. *Corros. Sci*., 2915(2005).